IARJSET

ISSN (O) 2393-8021, ISSN (P) 2394-1588

International Advanced Research Journal in Science, Engineering and Technology

Vol. 8, Issue 11, November 2021

DOI: 10.17148/IARJSET.2021.81119

PERFORMANCE SIMULATION OF STIRLING CRYOCOOLERS

Prof A. K. Madan[1] Abhishek Berwal[2] Aniket Yadav[3]

[1]Professor, Department of Mechanical Engineering, DTU, Delhi

[2]Research Scholar, Department of Production Engineering, DTU, Delhi

[3]Research Scholar, Department of Production Engineering, DTU, Delhi

Abstract: Small Stirling cryocoolers, with refrigeration capacities in the range of 0.5W to 5W, at cooling temperatures as low as 60K have found their way into the fields of aerospace, medical and energy. The present work is aimed at performance simulation of a Stirling cryocooler using CFD. Simulation of the reciprocating flow inside a 2-D model of the cryocooler has been accomplished using the dynamic mesh technique in ANSYS Fluent. For this purpose, two separate User Defined Functions (UDFs) have been compiled for the movement of piston and displacer. In order to operate the cryocooler based on the Stirling cycle an appropriate phase difference has been maintained between the piston and displacer movement. This model is time intensive but proves to be appropriate for cyclic simulations. The mesh inside the working spaces is compressed and expanded proportionally avoiding the negative volume error that is often encountered in moving mesh problems. Temperature-dependent properties of the working fluid and matrix material have been incorporated by using appropriate coefficients of polynomial functions as a function of temperature. Area weighted temperature and pressure inside the compression and expansion spaces have been reported for the ANSYS Fluent simulations. It is shown that the modelled cryocooler can achieve a refrigeration temperature of 60K with a heat load of 0.75W. The methodology adopted in the current work can be utilized to simulate the performance of a cryocooler and can be helpful in finding the optimum values of its operational parameters.

Keywords: Cryocoolers, ANSYS, Matrix, Aerospace industry

1. INTRODUCTION

Cryocoolers are the devices used to generate low temperature via expansion and compression of gas. It operates on a closed cycle manner, which means the mass of the working gas is constant. A cryocooler consists of a compressor, a heat exchanger and an expander. The cold generated in the expander is exchanged between the cold end and the object to be cooled using an evaporator. Cryocoolers are capable of producing temperatures as low as 77 K or 4.2 K are used to replace the cryogens (N2, He respectively).

Cryocoolers are usually categorized according to their inherent thermodynamic cycle, the heat exchange mechanism, cooling capacity, and most importantly the refrigeration temperature. They are designed for specific purposes and operate efficiently well for that particular cryogenic temperature range. Stirling cycle refrigerators using helium gas as the working fluid are widely used for a range of applications and remain the focus of this study. Military sensors that use cooled infrared semiconductor devices for heat source detection are of obvious importance in the fields of early warning systems and target identification etc. A considerable amount of research has been done on the regenerators and oscillatory internal flows. However, the approach adopted in this study is fairly straightforward, as it utilizes a built-in capability of the software (ANSYS Fluent) in order to address the moving mesh problem. The results obtained are in close conformance to the experimental results.

2. METHODOLOGY

A. FINITE VOLUME METHOD (FVM): The finite volume method is based on the integral form of conservation equations. The problem domain is divided into a set of non-overlapping control volumes (called finite volumes). The conservation equations are applied to each finite volume. The integrals occurring in the conservation equations are evaluated using function values at computational nodes (which are usually taken as centroids of finite volumes). This process involves use of approximate integral formulae and interpolation methods (to obtain the values of variables at surfaces of the CVs).

IARJSET

ISSN (O) 2393-8021, ISSN (P) 2394-1588

International Advanced Research Journal in Science, Engineering and Technology

Vol. 8, Issue 11, November 2021

DOI: 10.17148/IARJSET.2021.81119

The FVM can accommodate any type of grid, and hence, it is naturally suitable for complex geometries. This explains its popularity for commercial CFD packages, which must cater to problems in arbitrarily complex geometries. This method has immensely benefited from the unstructured grid generation methods developed for the finite element method.

Solution domain is sub-divided into a finite number of small control volume (CVs) by a grid. The grid defines the CV boundaries, not the computational modes. The integral conservation equation applies to each CV as well as to the solution domain as a whole. Thus, global conservation is built into the method. To obtain an algebraic equation for each CV, the surface and volume integrals are approximated using quadrature formulae. Thus, the overall finite volume solution process involves the following steps:

- Discretize the solution domain by a grid (i.e. a set of finite volumes), and define the computational nodes at which variables are to be evaluated.

- Apply the integral form of conservation law to each control volume. Approximate the surface and volume integrals using appropriate quadrature formulae in terms of the function values at computational nodes.

- Collect the algebraic equations for all the finite volumes to obtain a system of algebraic equations in terms of unknown values of the variable at computational nodes.

- Solve the resulting system of algebraic equations to obtain values of the variable at each computational node.

 TYPES OF FINITE VOLUME GRIDS

There are two common approaches to finite volume discretization: (a) cell-centred and (b) face centred grids (Figure a).

- Cell-centred approach: CVs are defined by a suitable grid (structured or unstructured) and computational nodes are assigned at the CV centre.

- Face-centred approach: Nodal locations are defined first, and CVs are then constructed around them so that CV faces lie midway between the nodes. It can be used only with structured grids. In view of its versatility, the first approach is most commonly employed.

Figure a: Types of FV grids: nodes centred in CVs (left) and CV faces centred between nodes (right)

B. COMPASS NOTATION

For structured Cartesian grids, compass notation is employed for computational nodes as shown in Figures b and c for 2-D and 3-D respectively. CV surfaces can be subdivided into 4 (in 2-D) or 6 (in 3-D) plane faces denoted by lower case letters corresponding to their direction (e, w, s, n, t and b) with respects to the central node P.

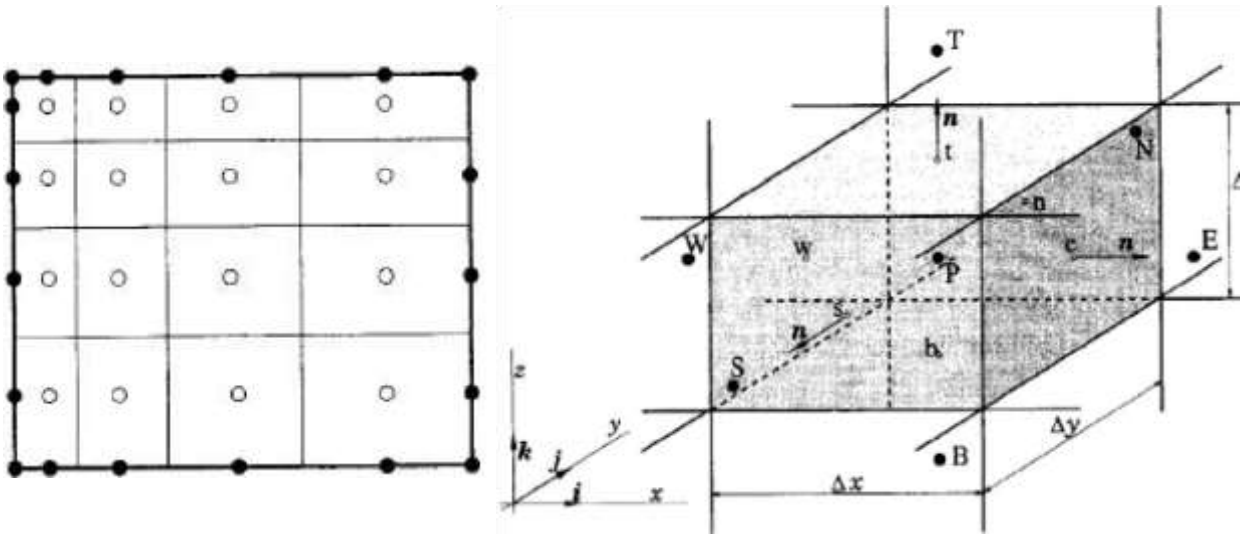

IARJSET

ISSN (O) 2393-8021, ISSN (P) 2394-1588

International Advanced Research Journal in Science, Engineering and Technology

Vol. 8, Issue 11, November 2021

DOI: 10.17148/IARJSET.2021.81119

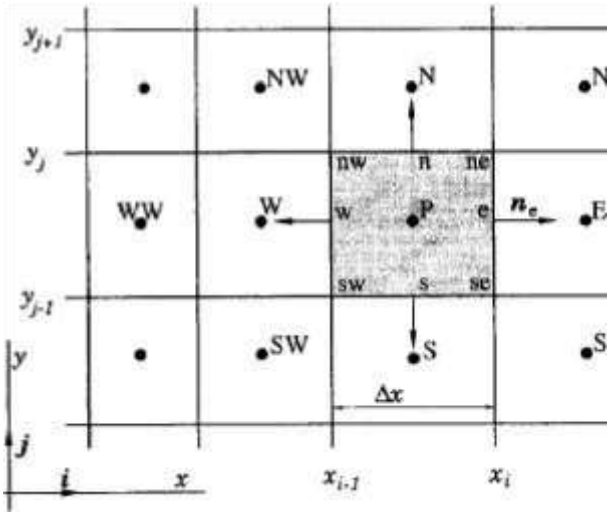

Figure b: A typical CV and notation used for 2D Cartesian finite volume grid

3. COMPUTATIONAL SETUP IN CFD

An important feature of transient analysis using dynamic mesh technique is the requirement of substantial computational power as well as time required to complete the simulations. Since this study involves only a 2-D model, the requirement of high computational power is relaxed. But the time required for completion of simulation still remains large and needs to be addressed appropriately. In order to deal with this factor it was decided to keep the mesh as simple as possible without losing a lot in terms of accuracy. All computations/simulations during the course of this study were performed on an Intel (R) Core i5-8265U 1.6 GHz with Turbo Boost up to 3.9 GHz that had a total installed RAM of 8GB. A typical layout of a split Stirling cryocooler is shown in Fig. 1. 2-D mesh, prepared in GAMBIT®, inside the compression space and expander assembly is shown in Fig.
2 and 3 respectively. A rectangular mesh is

used for all parts inside the system. An axisymmetric model of analysis can be used in such a scenario so only half of the model was created in GAMBIT® and meshing was applied to it.

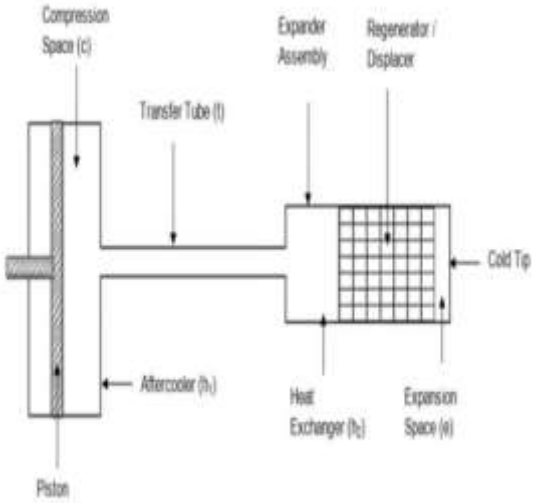

Fig. 1. Layout of a split Stirling cryocooler

There are three deforming zones: the compression space, the h2 space (a continuation of the compression space) and the expansion space. The mesh size in these zones was adjusted according to the size of each space and the requirement to

IARJSET ISSN (O) 2393-8021, ISSN (P) 2394-1588

International Advanced Research Journal in Science, Engineering and Technology

Vol. 8, Issue 11, November 2021

DOI: 10.17148/IARJSET.2021.81119

have a perfectly square mesh-cell when the piston reaches the centre of its displacement length. The following figures represent the cryocooler at the start of the simulation.

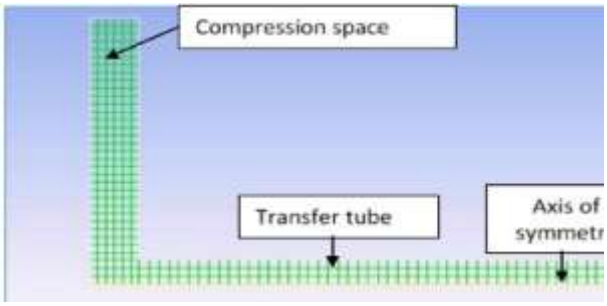

Fig. 2. Mesh inside the compression space

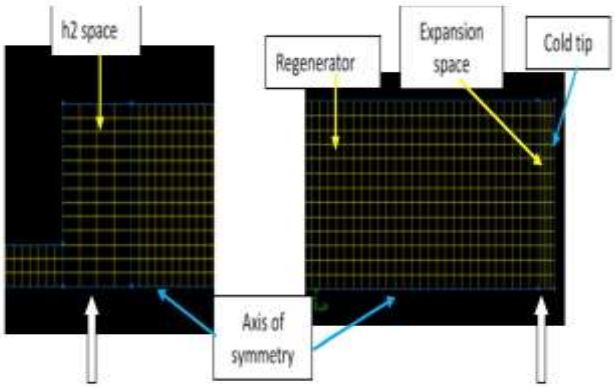

Fig. 3. Mesh inside the expander assembly

Mesh and time independence study was carried out with the fine mesh being the obvious winner in terms of accuracy, when compared with the experimental results. However, it required substantially high solution time (Table 1). The flow time of 28 seconds in ANSYS Fluent corresponded to more than 40 days of real-life time. Therefore, a medium quality mesh was chosen to achieve a solution in a reasonable time (almost 22 days), without having to lose a lot of accuracy.

Mesh Type	No. of Nodes	Expansion Space Temperature (K)	Flow Time for Solution (Sec)
Coarse Mesh	2916	42.5	12
Medium Mesh	5133	60.7	17
Fine Mesh	10060	64	28

Table 1

The mesh file prepared in GAMBIT® was imported to ANSYS Fluent® after properly defining the various walls and zones. The solid

part of the system is made up of Stainless Steel (SS) whereas the working fluid is Helium gas. The initial charging pressure and the ambient temperature are chosen according to the design requirement. The heat load at coldtip is specified once required, otherwise for the no-load case the cold-tip is assumed as adiabatic wall.

STEPS solving problem in ANSYS FLUENT

To solve engineering problems using ANSYS FLUENT the necessary steps are:

 Pre-Analysis : In the Pre-Analysis step, we'll review the following:

IARJSET ISSN (O) 2393-8021, ISSN (P) 2394-1588

International Advanced Research Journal in Science, Engineering and Technology

Vol. 8, Issue 11, November 2021

DOI: 10.17148/IARJSET.2021.81119

- **Mathematical model:** We'll look at the governing equations + boundary conditions and the assumptions contained within the mathematical model.

- **Numerical solution procedure in Ansys :** We'll briefly overview the solution strategy used by Ansys and contrast it to the hand calculation approach.

➢ **Geometry** : Geometry modeling in the Ansys Workbench environment is highly automated and also provides users the flexibility to customize according to the type of analysis or application. The feature-based, parametric Ansys DesignModeler software can be used to create parametric geometry from scratch or to prepare an existing CAD geometry for analysis. It includes automated options for simplification, cleanup, repair and defeaturing.

➢ **Mesh:** Ansys Fluent meshing is a powerful tool, which can be **used to achieve high-quality and accurate measures** for your 3D geometries. Let's take a minute to elaborate on some of the capabilities and features that you stand to gain when using Fluent meshing.

➢ **Physical setup:** It is done in the solver ANSYS. In this step you give inputs for solution accuracy, boundary condition, physics involved, material involved, properties involved etc. **Numerical solution**

Verification and Validation:

Verification and validation **examines the errors in the code and simulation results**. Credibility is obtained by demonstrating acceptable levels of uncertainty and error. A discussion of the uncertainties and errors in CFD simulations is provided on the page entitled Uncertainty and Error in CFD Simulations.

Two User Defined Functions (UDFs) for the sinusoidal motion of piston and displacer/regenerator have been compiled in C++ to provide the necessary motion at an appropriate phase difference inside the Fluent environment. The UDFs are applied to the piston in compression space and all the sides of the regenerator as well as the fluid zone inside the regenerator. The top and bottom sides in h2 space and expansion space are set as deforming, to accommodate for the sinusoidal motion of the regenerator. The motion of the regenerator causes an equal amount of change in volume for the expansion space and the h2 space but in the opposite directions. For example, if the regenerator moves towards the cold tip the expansion space is compressed whereas the volume inside h2 space is expanded. The temperature dependant properties of Helium and Stainless Steel are provided as polynomial functions inside ANSYS Fluent® based on an empirical curve fit over the experimental data available on the website of National Institute of Standards and Technology. Necessary details about the cryocooler are shown in Table 2.

Initial Charging Pressure	35 bars
Rotation Speed	2700
Transfer Tube Length	150 mm
Piston Stroke Length	2 mm
Internal Diameter of Compression Cylinder	17 mm

Table 2

The solver settings in ANSYS Fluent are shown in Table III whereas the boundary conditions are shown in Table IV. The walls of the transfer tube and heat exchanger are assumed to be isothermal, considering that the cryocooler is designed to operate at standard room temperature. Viscous resistance and inertial loss coefficient of the regenerator are calculated using its dimensions and porosity.

Analysis type	2D axi-symmetric
Solver	Pressure based
Time	Transient
Viscous model	Standard k-epsilon
Material	Fluid: Helium, Matrix: Stainless Steel (SS)
Cell Zone condition	Regenerator: Porous Media

IARJSET

ISSN (O) 2393-8021, ISSN (P) 2394-1588

International Advanced Research Journal in Science, Engineering and Technology

Vol. 8, Issue 11, November 2021

DOI: 10.17148/IARJSET.2021.81119

Dynamic Mesh	Smoothing: Linearly elastic solid
Pressure velocity coupling	PISO

Piston	Stainless Steel, Adiabatic
Compression space walls	SS, Adiabatic
Transfer Tube	SS, Isothermal at 300K
Heat Exchanger (h2)	SS, Deforming, Isothermal at 300k
Regenerator	Porous medium, SS, Adiabatic mesh size = 0.25mm, Porosity = 0.7 Viscous Resistance Constant: X= 3.086e+08m-2, Y= 3.086e+08m-2 Inertial loss coefficient: X= 12244.9 m-1, Y= 12244.9 m-1
Expansion space walls	SS, Deforming, Adiabatic
Cold-tip	SS, Adiabatic for noload condition
Fluid	Helium gas with temperature dependent properties

4. RESULTS AND DISCUSSION

Area averaged temperature and pressure were recorded for the compression and expansion spaces. Fig. 4 shows the variation of compression space pressure with flow time. The maximum pressure reached is almost 3.3E+06Pa whereas the minimum pressure is 2E+06Pa. The expansion space pressure variation is shown in Fig. 5. Because of the pressure drop mainly due to the regenerator, the effective pressure inside the expansion space is much less than the compression space. It only achieves a maximum pressure of approximately 2.9E+06Pa. The variation of compression space temperature with flow time for the initial part of the simulation is shown in Fig. 6. The temperature is seen to gradually rise from 300K to almost 330K. Fig. 7 shows the variation of temperature in expansion space for the initial part of the simulation. The temperature decreases quickly with the passage of time as can be easily seen from the figure.

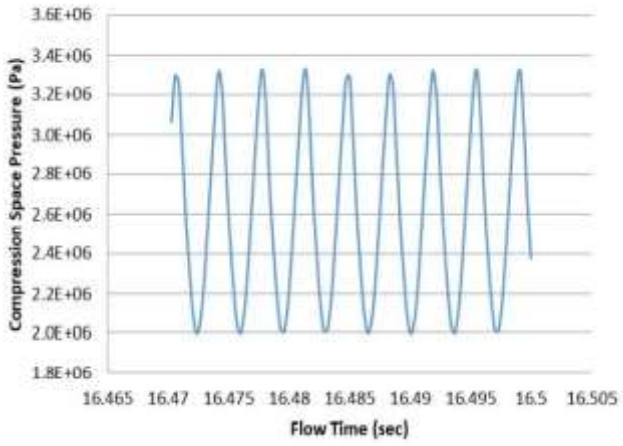

Fig. 4. Compression space pressure vs. flow time

IARJSET

ISSN (O) 2393-8021, ISSN (P) 2394-1588

International Advanced Research Journal in Science, Engineering and Technology

Vol. 8, Issue 11, November 2021

DOI: 10.17148/IARJSET.2021.81119

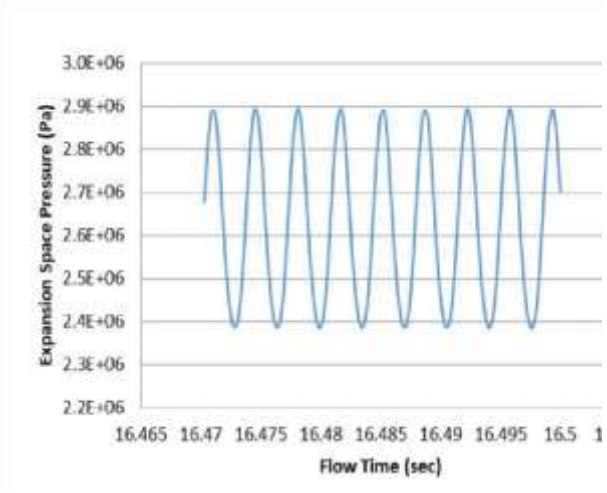

Fig. 5. Expansion space pressure vs. flow time

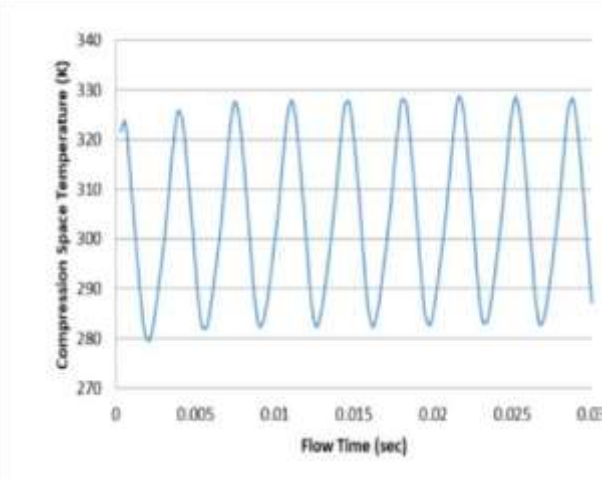

Fig. 6. Compression space temperature vs. flow time

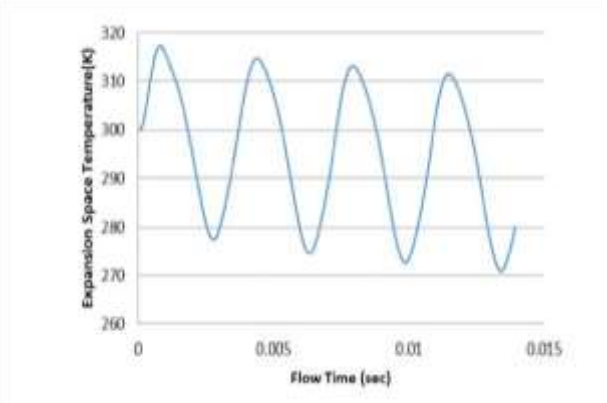

Fig. 7. Expansion space temperature vs. flow time

during the cycle at approximately 15 seconds of flow time. It is visible from Fig. 8 that the cryocooler is capable of achieving approximately 60K at the cold end.

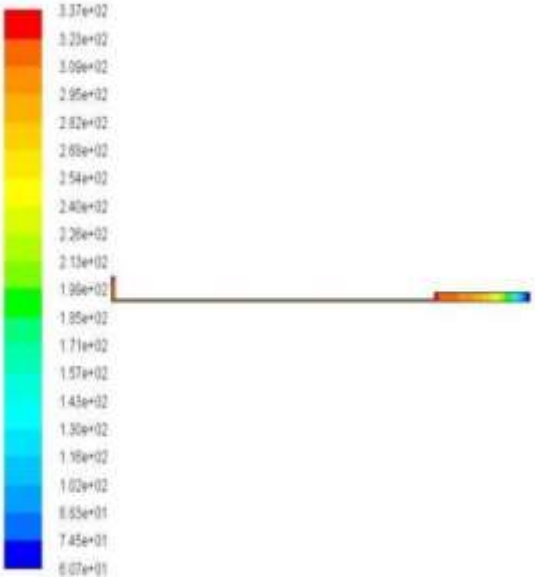

Fig. 8. Contours of static temperature inside cryocooler

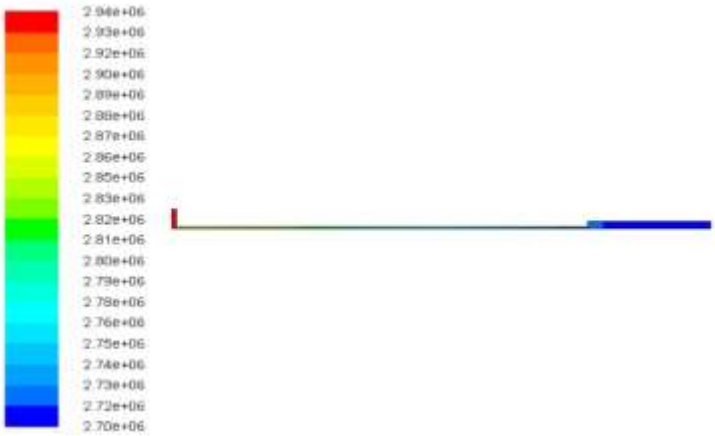

Fig. 9. Contours of static pressure inside cryocooler

The cool down behaviour of a cryocooler is one of the primary factors for its preliminary design. The simulations in ANSYS Fluent were therefore directed towards finding the time variation of temperature inside the expansion space of the cryocooler for different scenarios. The following figure shows a comparison between the simulated and experimental results of the cool down behaviour of the cryocooler. The simulations were run for seventeen seconds of flow time. The temperature drop is quite substantial for the first ten

IARJSET ISSN (O) 2393-8021, ISSN (P) 2394-1588

International Advanced Research Journal in Science, Engineering and Technology

Vol. 8, Issue 11, November 2021

DOI: 10.17148/IARJSET.2021.81119

seconds of the simulation time. Afterwards, the decrease in temperature is very less and shows an almost asymptotic behaviour.

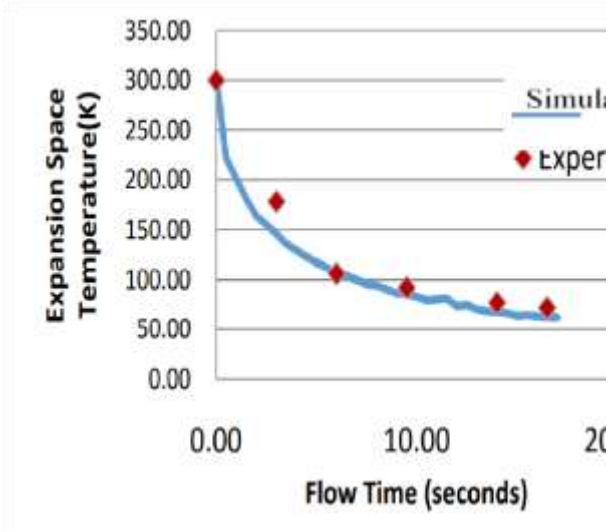

Fig. 10. Cool down curve of the cryocooler

5. CONCLUSION

The CFD simulation result shows that the cryocooler is expected to successfully achieve the desired refrigeration temperature of 60K with a heat load of 0.75W. The results are optimistic by almost 8% when compared with the experimental data. The difference exists because of the assumptions taken in the formulation of the problem in ANSYS Fluent. Since the model is 2-D, it does not include the 3-D interference effects that occur due to the interaction of the flow between the solid parts of the cryocooler. Additionally, the boundary conditions were such that some of the parts are maintained at 300K throughout the period of simulation which is difficult to achieve in real world. Furthermore, the wall thickness and thus the conduction losses of the cryocooler have not been considered in the model. However, the present study will help us in formulation of a 3-D model of the cryocooler and therefore better handling of the conduction and shuttle heat loss phenomenon which have not been included in the current model. These effects are expected to increase the expansion space temperature. Moreover, a parametric study of the effect of various input parameters on the cryocooler performance will also be undertaken as a future task.

REFERENCES

[1] H. S. et al, “Miniature Cryogenic Coolers,” Advances in cryogenic engineering, 1976.
[2] B. Ibrahim and W. Simon, “CFD Modelling of Free-Piston Stirling,” no. September 2001, 2018.
[3] D. Gedeon, “Sage Object Oriented Software for Cryocooler Design,” 1995.
[4] G. Y. Yu, W. Dai, J. Qiu, L. M. Zhang, X. W. Li, and B. Liu, “Initial Test of a Stirling Cryocooler with a High Cooling Capacity,” in International Cryocooler Conference 18, 2014, pp. 169–175.
[5] K. Yumoto, K. Nakano, and Y. Hiratsuka, “Development of high capacity split stirling cryocooler for HTS,” Phys. Procedia, vol. 67, no. 2013, pp. 462–467, 2015.
[6] A. Caughley, M. Sellier, M. Gschwendtner, and A. Tucker, “CFD analysis of a diaphragm free-piston Stirling cryocooler,” Cryogenics (Guildf)., vol. 79, pp. 7–16, 2016.
[7] A. Alexakis, “CFD Modelling of Stirling Engines with Complex Design Topologies,” University of Northumbria at Newcastle, 2013.
[8] A. R. and Barrett Flake, “Modelling Pulse Tube Cryocooler with CFD.pdf,” Advances in Cryogenic Engineering Vol. 49, pp. 1493–1499, 2004.
[9] Y. et al, “Computational Fluid Dynamic Modelling of Pressure Drop through Wire Mesh Screen Regenerators,” A[10] Babcock, G. H. (1885). “Substitutes for Steam.” *ASME Trans*. **7**, 680–741.
[11] Beale, W. (1979). Private Communication. Sunpower Inc., Athens, Ohio.
[12] Berchowitz, D. M., Rallis, C. J., and Urieli, I. (1977). “A New Mathematical Model for Stirling Cycle Machine.” Proc. 12th I.E.C.E.C., pp. 1522-1527, Washington, D.C., August 28– September 2.
[13] Cairelli, J. E., and Thieme, L. G. (1977). “Initial Test Results with a Single Cylinder Rhombic Drive Stirling Engine.” Proc. ERDA, Highway Veh. Syst. Cont. Coord. Mtg., Dearborn, Michigan, October 4-6.
[14] Chellis, F., and Stewart, R. W. (1972). “Multiple Cold Finger Refrigeration System for

IARJSET ISSN (O) 2393-8021, ISSN (P) 2394-1588

International Advanced Research Journal in Science, Engineering and Technology

Vol. 8, Issue 11, November 2021

DOI: 10.17148/IARJSET.2021.81119

Cooling Infra-Red Detectors." AFFDL-TR-72-84, AD No. 903-939L (Cryogenic Technology Inc., Latham, Massachusetts).
[15] Collins, S. C, and Cannaday, R. L.
(1958). *Expansion Machines for Low Temperature Processes*. Oxford University Press, Oxford.
[16] Daniels, A., and du Pre, F. K. (1971). "Triple-Expansion Stirling Cycle Refrigerator." *Adv. Cryog. Eng*. **16**, 178–184.
[17] de Jonge, A. K. (1979). "A Small FreePiston Stirling Refrigerator." Paper No. 799245, pp. 1136–1141, Proc. 14th I.E.C.E.C., Boston, Massachusetts.
[18] Dros, A. A. (1965). "An Industrial Gas
Refrigerating Machine with Hydraulic Piston Drive." *Philips Tech. Rev*. **26**(10), 297–306.
[19] Finegold, J. G., and Vanderbrug, T. G. (1977). Stirling Engines for Undersea Vehicles." Final Report No. 5030-63, J.P.L., March.
IP Conf. Proc., vol. 710, no. 2004, pp. 1138– 1145, 2004.
[20] Finkelstein, T. (1959). "Air Engines." *Engineer* **207**, 492–497, 522-527, 568-571, 720-723.
[21] Finkelstein, T. (1959). "Development and
Testing of a Stirling Cycle Machine with
Characteristics Suitable for Domestic Refrigeration." English Electric Report W/M/3A.
[22] Finkelstein, T. (1960). "Generalized Thermodynamic Analysis of Stirling Engines." S.A.E. Paper No. 118B, January.
[23] Finkelstein, T., Walker, G., and Joshi, T.
(1970). "Design Optimization of Stirling-Cycle
Cryogenic Cooling Engines by Digital Simulation." Cryog. Eng. Conf., Paper K4, Boulder, Colorado, June.
[24] Finkelstein, T. (1975). "Computer Analysis of Stirling Engines." *Adv. Cryog. Eng*. **20**, 269– 282
[25] Finkelstein, T. (1978). "Modeling Design and Optimization of Stirling Engines." Proc. 13th I.E.C.E.C, San Diego, California, August 20–25.
[26] Finkelstein, T. (1978). Pressure Compounding of Stirling Engines. Proc. 13th I.E.C.E.C, San Diego, California.
[27] Gedeon, D. (1978). "Optimization of Stirling Cycle Machines." Proc. 13th I.E.C.E.C, San Diego, California.
[28] Goldwater, B., and Morrow, R. B. (1977). "Demonstration of a Free Piston Stirling Linear Alternator Power Conversion System." Proc. 12th I.E.C.E.C, Paper No. 779249, pp.1488– 1495, Washington, D. C, August 28– September 2.
[29] Haarhuiss, G. J. (1978). "The MC 80—A
Magnetically Driven Stirling Refrigerator." Proc. 7th Int. Cryog. Eng. Conf., London, IPC Business Press, Guildford, U.K.
[30] Higa, W. N. (1965). "A Practical Philips
Cycle for Low Temperature Refrigeration." *Cryog. Technol*. 8, 203–209, July–August.
[31] Horn, S. B., Lumpkin, M. L., Walters, B. T., and Acord, T. T. (1973). "Miniature Cryogenic Cooler for TOW Night Sight." Proc. Closed Cycle Cryocooler Tech. and Appl., Vol. 1, pp. 55–72, AFFDL-TR-73-149, WPAFB, Ohio, AD No. 918234.
[32] Khan, M. I. (1962). "The Application of Computer Techniques to the General Analysis of the Stirling Cycle." M.Sc. thesis, Univ. of Calgary.
[33] Kirk, A. (1874). "On the Mechanical Production of Cold." *Proc. Ins. Civil Eng*. **37**, 244–315, London.
[34] Köhler, J. W. L. (1965). The Stirling Refrigeration Cycle. *Sci. Am*. **212**(4), 119–127.
[35] Lee, K. (1976). "The Stirling Cycle with Adiabatic Compression and Expansion." M.Sc. thesis, Univ. of Calgary.
[36] Lindale, E. (1978). "Stirling Cycle
Refrigerators for Gamma Ray Detector."
Report No. PL-42-Cr78-0713, Johns Hopkins Univ., Applied Physics Lab., Laurel, Maryland (Philips Laboratories).
[37] Maki, E. R., and de Hart, A. O. (1971). "A
New Look at Swash-Plate Drive Mechanisms."
S.A.E. Trans. (Truck, Powerplant Fuels and Lubricants Mtg.), Vol. 80, Paper No. 710829, St. Louis, Missouri, October.
[38] Martini, W. (1978). Design Manual for
Stirling Engines. NASA CR 135382, DOE/NASA Contractor Report (NTIS, Springfield, Virginia). See also: Stirling Engine Design and Feasibility for Automotive Use. (1979). (ed. M. J. Collie), Noyes Data Corp., Park Ridge, New Jersey.
[39] Prast, G. (1963). "A Philips Gas Refrigerating Machine for 20 K." *Cryogenics* **3**, 156–160, September.
[40]Prast, G. (1965). "A Gas Refrigerating
Machine for Temperatures down to 20 K and
Lower." *Philips Tech. Rev*. **26**(1), 1–11, January